

# A Dual Quaternion Framework for Collision Recovery of Quadrotor

Valentin Gaucher and Wenlong Zhang

**Abstract**—Unmanned aerial vehicles (UAVs) operating in cluttered environments require accurate impact modeling to maintain stability. However, conventional contact models decouple linear and angular impulses, risking manifold inconsistency during rapid state transitions. This article presents a dual quaternion reset map that resolves rigid-body impacts directly on the  $SE(3)$  manifold. By operating on the unified spatial twist (linear and angular velocities as a single dual entity), our formulation is algebraically equivalent to the classical Newton impulse model while preserving manifold consistency during discrete state jumps. Building on this framework, we design a hybrid recovery controller that couples linear and angular momentum to ensure strict energy dissipation across impacts. Hardware-in-the-loop benchmarks demonstrate a 24% reduction in execution latency compared to an optimized matrix-based implementation. High-fidelity MuJoCo simulations validate the controller’s robustness to complex contact dynamics, showing a 56.6% reduction in post-impact root-mean-square error (RMSE) and a 41.2% decrease in peak kinetic energy compared to decoupled recovery methods.

**Index Terms**—Aerial Systems, Hybrid Systems, Dual Quaternions, Collision Recovery

## I. INTRODUCTION

### A. Motivation and Problem Statement

Unmanned aerial vehicles (UAVs) are increasingly deployed in cluttered environments which necessitate collision recovery following physical interactions for stabilization [1] and tactile-based exploration [2]. In such settings, accurate modeling of impact-induced state discontinuities is essential for designing the recovery controllers. These collision events are inherently hybrid: the vehicle’s states evolve continuously on the configuration manifold  $SE(3)$  during free flight, and undergo instantaneous jumps in spatial velocity upon contact. Ensuring consistency of these discrete resets with the underlying geometric structure is critical for closed-loop stability.

Classical rigid-body impact models are derived from Newton impulse-momentum principles. They are typically implemented using rotation matrices with decoupled translational and rotational coordinates [3]. While physically correct, resolving discrete impacts in separate spaces ( $\mathbb{R}^3 \times SO(3)$ ) becomes problematic because a single physical contact force instantaneously couples linear and angular momentum. Calculating these discrete jumps separately often leads to practically inconsistent post-impact states forcing the system to apply artificial normalizations or projections to reconcile the state with physical constraints [4]. These corrections act as unmodeled disturbances that inject artificial energy into the system, complicating geometric controller design.

This work is supported by National Science Foundation under Grant No. 2331781.

The authors are with School of Manufacturing Systems and Networks, Ira A. Fulton Schools of Engineering, Arizona State University, Mesa, AZ, 85212, USA. Email: {vgaucher, wenlong.zhang}@asu.edu.

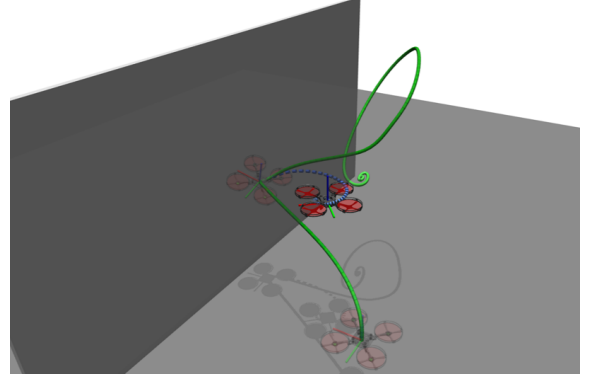


Fig. 1: UAV collision recovery performance in MuJoCo simulation. The proposed Dual Quaternion framework (blue, dashed) effectively mitigates linear and angular state oscillations post-impact, preventing drift seen in the traditional matrix-based approach (green, solid).

To address this challenge, we develop a reset map directly on the dual quaternion representation of  $SE(3)$ , enabling impact resolution on a unified spatial algebra. The proposed formulation extends Newton’s restitution law to dual screws and updates the twist in a closed form. The post-impact states remain on the valid manifold of rigid-body motion without the need for secondary algebraic corrections, capturing the physical cross-coupling of impact forces.

### B. Related Work

The mathematical foundation for rigid-body impacts is well-established, with the impulse-based approach to simultaneous collision resolution [5] providing the foundations for modern work such as a high-speed recovery controller for a quadrotor based on the classical matrix-based formulation to estimate post-impact states [3]. Existing work also models impacts by solving linear complementarity problems (LCP) in the inertial frame [6], and remains a valuable choice in the field of robotics, such as MuJoCo contact solving software [7] or recent work developing an LCP contact model for UAVs [8].

Parallel to these developments, dual quaternions have emerged as a superior alternative to matrix algebra for UAV flight control. First introduced by Clifford [9], dual quaternions offer a compact, singularity-free representation of 6-DOF motion by mapping the group of rigid-body transformations  $SE(3)$  to the unit dual quaternion manifold. We refer the reader to [10] for practical examples. This allows for the simultaneous representation of rotation and translation as a single screw displacement, eliminating the need for decoupled coordinate frames. Several works have demonstrated that dual quaternion-based control laws offer superior computational

efficiency compared to matrix-based approaches [11]. It is also shown that dual quaternions allow for control laws that couple rotation and translation into a single, singularity-free operation making them more efficient and numerically stable than their matrix counterparts [12]. Therefore, they have been widely used for trajectory tracking [13]–[15].

Despite these advances, dual quaternions have not been studied for hybrid modeling of UAV collisions. Recovery frameworks like [3] rely on classical matrix-based physics that resolve impacts in decoupled translational and rotational spaces. This introduces a sequence of state transformations which not only incurs unnecessary computational overhead but also introduces numerical errors. By forcing a discrete jump across disparate coordinate representations, these methods fail to capture the intrinsic coupling of impact forces, leading to suboptimal recovery responses.

### C. Contributions

In this paper, we derive a closed-form hybrid reset map on the dual quaternion representation of  $SE(3)$  for rigid-body impacts. By resolving impulse-momentum dynamics directly in dual algebra, our formulation updates the unified spatial twist while guaranteeing manifold-consistent state jumps, proving algebraically equivalent to classical impulse models. Building on this, we develop a collision recovery controller with proven Hybrid Lyapunov stability. This controller couples linear and angular momentum to dissipate impact energy (see Fig. 1) and integrates with standard cascaded architectures. Finally, we demonstrate that this approach yields practical computational advantages, including reduced embedded execution latency and superior robustness to asymmetric contact disturbances in high-fidelity UAV simulations.

## II. PRELIMINARIES

### A. Notation and Algebra

Let  $\mathcal{F}_W$  and  $\mathcal{F}_B$  denote the inertial and body frames, respectively. The set of unit quaternions is  $\mathbb{S}^3 \subset \mathbb{H}$  where  $\mathbb{H}$  is the quaternion space. For any vector  $\mathbf{v} \in \mathbb{R}^3$ , we associate it with a pure quaternion in  $\mathbb{H}_p$ , and a rotation of  $\mathbf{v}$  by  $\mathbf{q} \in \mathbb{S}^3$  is written as  $\mathbf{q} \odot \mathbf{v} = \mathbf{q} \otimes \mathbf{v} \otimes \mathbf{q}^*$ , where  $(\cdot)^*$  is the conjugate operation and  $\otimes$  is the quaternion multiplication. The algebra of dual quaternions  $\mathcal{H}_d$  uses dual numbers  $\hat{\mathbf{a}} = \mathbf{a} + \varepsilon \mathbf{b}$ , where  $\varepsilon$  is the nilpotent unit ( $\varepsilon^2 = 0, \varepsilon \neq 0$ ). The fundamental dual operations dot product  $\langle \cdot, \cdot \rangle$ , cross product ( $\times$  for kinematics) and adjoint cross product ( $\times^*$  for kinetics) are defined as:

$$\begin{aligned} \langle \mathbf{a} + \varepsilon \mathbf{b}, \mathbf{c} + \varepsilon \mathbf{d} \rangle &= \mathbf{a} \cdot \mathbf{c} + \mathbf{b} \cdot \mathbf{d} \\ (\mathbf{a} + \varepsilon \mathbf{b}) \times (\mathbf{c} + \varepsilon \mathbf{d}) &= \mathbf{a} \times \mathbf{c} + \varepsilon (\mathbf{a} \times \mathbf{d} + \mathbf{b} \times \mathbf{c}) \\ (\mathbf{a} + \varepsilon \mathbf{b}) \times^* (\mathbf{c} + \varepsilon \mathbf{d}) &= (\mathbf{a} \times \mathbf{c} + \mathbf{b} \times \mathbf{d}) + \varepsilon (\mathbf{a} \times \mathbf{d}) \end{aligned}$$

Additionally, for a dual matrix  $\hat{\mathbf{K}} = \mathbf{A} + \varepsilon \mathbf{B}$  and dual vector  $\hat{\mathbf{a}}$ , we use the decoupled matrix multiplication  $\circ$  as  $\hat{\mathbf{K}} \circ \hat{\mathbf{a}} = \mathbf{A}\mathbf{a} + \varepsilon \mathbf{B}\mathbf{b}$ . Those definitions can be found here [12].

### B. Standard Quaternion Flight Dynamics

The state of the UAV is defined by  $(\mathbf{p}^W, \mathbf{v}^W, \mathbf{q}, \boldsymbol{\omega}^B)$ , where  $\mathbf{p}^W \in \mathbb{R}^3$  and  $\mathbf{v}^W \in \mathbb{R}^3$  are the position and linear velocity in  $\mathcal{F}_W$ ,  $\mathbf{q} \in \mathbb{S}^3$  is the unit quaternion representing the orientation of  $\mathcal{F}_B$  relative to  $\mathcal{F}_W$ , and  $\boldsymbol{\omega}^B \in \mathbb{R}^3$  is the angular velocity in  $\mathcal{F}_B$ . The continuous-time dynamics are:

$$\begin{aligned} \dot{\mathbf{p}}^W &= \mathbf{v}^W, \quad \dot{\mathbf{q}} = \frac{1}{2} \mathbf{q} \otimes \boldsymbol{\omega}^B \\ \dot{\mathbf{v}}^W &= g \mathbf{e}_z^W - \frac{f}{m} \mathbf{q} \odot \mathbf{e}_z^B, \quad \mathbf{J} \dot{\boldsymbol{\omega}}^B = \boldsymbol{\tau}^B - \boldsymbol{\omega}^B \times (\mathbf{J} \boldsymbol{\omega}^B) \end{aligned} \quad (1)$$

where  $m \in \mathbb{R}^+$  is the mass,  $\mathbf{J} \in \mathbb{R}^{3 \times 3}$  is the constant positive-definite inertia matrix,  $f \in \mathbb{R}$  is the total thrust, and  $\boldsymbol{\tau}^B \in \mathbb{R}^3$  is the control torque in  $\mathcal{F}_B$ .

### C. Matrix-Based Reset Model

Here, we review the standard impulse-momentum impact model [3], [5]. Let the impact occur at point  $\mathbf{r}_c$  (body frame) with normal  $\mathbf{n}$  (world frame). The post-impact state  $(\mathbf{v}^+, \boldsymbol{\omega}^+)$  is given by the mapping  $\mathcal{R}$ :

$$\mathcal{R} : \begin{cases} \mathbf{v}^+ &= \mathbf{v}^- + m^{-1} \boldsymbol{\lambda} \\ \boldsymbol{\omega}^+ &= \boldsymbol{\omega}^- + \mathbf{J}^{-1} (\mathbf{r}_c \times (\mathbf{R}^\top \boldsymbol{\lambda})) \end{cases} \quad (2)$$

where  $\boldsymbol{\lambda}$  is the impulse vector and  $\mathbf{R} = \mathbf{R}(\mathbf{q})$  is the rotation matrix. The impulse magnitude is derived from the effective mass  $\rho$  as follows:

$$\boldsymbol{\lambda} = - \frac{(1+e) \mathbf{v}_c^{-\top} \mathbf{n}}{\rho} (\mathbf{n} + \mu \mathbf{t}) \quad (3a)$$

$$\rho = m^{-1} + \mathbf{n}^\top \mathbf{R} [\mathbf{J}^{-1} (\mathbf{r}_c \times (\mathbf{R}^\top \mathbf{n})) \times \mathbf{r}_c] \quad (3b)$$

where  $\mathbf{v}_c = \mathbf{v} + \mathbf{R}(\boldsymbol{\omega} \times \mathbf{r}_c)$  is the pre-impact velocity,  $e$  the restitution coefficient and  $\mu$  the friction coefficient. The vectors  $\mathbf{n}$  and  $\mathbf{t}$  are the normal and tangential vectors at the impact point in  $\mathcal{F}_W$ .

## III. DUAL QUATERNION FORMULATION

### A. Dual Quaternion Flight Dynamics

We represent the UAV configuration on  $SE(3)$  using a unit dual quaternion  $\hat{\mathbf{q}} \in \mathcal{H}_d$ , providing a global, non-singular mapping of the translational position  $\mathbf{p} \in \mathbb{R}^3$  and orientation  $\mathbf{q} \in \mathbb{S}^3$ . The velocities are encapsulated by the dual twist  $\hat{\boldsymbol{\xi}} \in \mathcal{H}_d^p$ , a pure dual quaternion composed of the body-frame angular velocity  $\boldsymbol{\omega} \in \mathbb{R}^3$  and linear velocity  $\mathbf{v}_B \in \mathbb{R}^3$ . We formalize the dual dynamics, denoted  $F$ , below [13]–[15]

$$\begin{aligned} \hat{\mathbf{q}} &= \mathbf{q} + \varepsilon \left( \frac{1}{2} \mathbf{p} \otimes \mathbf{q} \right), \quad \hat{\boldsymbol{\xi}} = \boldsymbol{\omega} + \varepsilon \mathbf{v}_B, \\ \dot{\hat{\mathbf{q}}} &= \frac{1}{2} \hat{\mathbf{q}} \otimes \hat{\boldsymbol{\xi}}, \quad \dot{\hat{\boldsymbol{\xi}}} = \mathcal{M}^{-1} (\hat{\mathbf{F}} - \hat{\boldsymbol{\xi}} \times^* \hat{\mathbf{H}}), \end{aligned} \quad (4)$$

where  $\mathbf{v}_B = \mathbf{q}^* \odot \mathbf{v}$  and  $\hat{\mathbf{H}}$  is the dual momentum [16] defined via the dual inertia operator  $\mathcal{M} : \mathcal{T}_{\hat{\mathbf{q}}} \mathcal{H}_d \rightarrow \mathcal{T}_{\hat{\mathbf{q}}}^* \mathcal{H}_d$  mapping the tangent space (velocities) to the cotangent space (forces/momenta) at the center of mass. Applying this operator to the twist gives the dual momentum:

$$\hat{\mathbf{H}} = \mathcal{M}(\hat{\boldsymbol{\xi}}) = \mathbf{J} \boldsymbol{\omega} + \varepsilon (m \mathbf{v}_B) \quad (5)$$

In the body frame, the operator  $\mathcal{M}$  is constant and its inverse is exactly defined as:

$$\mathcal{M}^{-1}(\hat{\xi}) = \mathbf{J}^{-1}\boldsymbol{\omega} + \varepsilon(m^{-1}\mathbf{v}_B). \quad (6)$$

$\hat{\mathbf{F}} = \hat{\mathbf{F}}_a + \hat{\mathbf{F}}_g$  represents the total external dual wrench acting on the UAV CoM, expressed in the body frame.  $\hat{\mathbf{F}}_a$  (thrust and torque) and the gravitational wrench  $\hat{\mathbf{F}}_g$  can be written as

$$\hat{\mathbf{F}}_g = \mathbf{0} + \varepsilon\mathbf{q}^* \odot (m\mathbf{g}), \quad \hat{\mathbf{F}}_a = \boldsymbol{\tau} + \varepsilon\mathbf{f}, \quad (7)$$

with  $\mathbf{f} \in \mathbb{R}^3$  the thrust vector.

### B. The Dual Quaternion Reset Map

**Assumption 1.** The collision between the UAV and the environment is modeled as a perfectly rigid impact over an infinitesimally small time interval. The configuration of the UAV remains continuous across the impact event ( $\hat{\mathbf{q}}^+ = \hat{\mathbf{q}}^-$ ).

We propose a dual quaternion (DQ) reset map  $\hat{\mathcal{R}}$  that operates exclusively on the spatial twist  $\hat{\xi}$ . Unlike classical formulations that require intermediate mappings out of the configuration space to  $SO(3)$  rotation matrices to resolve collisions, our approach evaluates the impact within the dual algebra. This preserves the  $SE(3)$  geometry across the discrete jump while rigorously satisfying the physics. Under Assumption 1, the impact law relates the discrete jump in dual momentum  $\hat{\mathbf{H}}$  to the external impulsive wrench  $\hat{\mathcal{W}}$  acting on the system as follows:

$$\Delta\hat{\mathbf{H}} = \hat{\mathbf{H}}^+ - \hat{\mathbf{H}}^- = \hat{\mathcal{W}}. \quad (8)$$

Substituting the algebraic relationship  $\hat{\mathbf{H}} = \mathcal{M}(\hat{\xi})$ , we obtain the following dual quaternion reset map:

$$\hat{\mathcal{R}} : \hat{\xi}^+ = \hat{\xi}^- + \mathcal{M}^{-1}(\hat{\mathcal{W}}). \quad (9)$$

The impact geometry is defined by the contact point  $\mathbf{r}_c$  and the surface normal  $\mathbf{n} \in \mathbb{R}^3$ . To maintain coordinate invariance, we transform the world-frame normal to the body frame using the current attitude  $\mathbf{q}$  with  $\mathbf{n}_B = \mathbf{q}^* \odot \mathbf{n}$ . We define the collision geometry using two orthogonal unit screws in Plücker line coordinates [10], namely the normal screw  $\hat{\mathbf{s}}_n \in \mathcal{H}_d$  (penetration) and the tangential screw  $\hat{\mathbf{s}}_t \in \mathcal{H}_d$  (slip):

$$\hat{\mathbf{s}}_n = (\mathbf{r}_c \times \mathbf{n}_B) + \varepsilon\mathbf{n}_B, \quad \hat{\mathbf{s}}_t = (\mathbf{r}_c \times \mathbf{t}_B) + \varepsilon\mathbf{t}_B, \quad (10)$$

where  $\mathbf{t}_B$  is the unit vector in the direction of the sliding velocity. We model the total collision wrench  $\hat{\mathcal{W}}$  by applying a normal impulse (magnitude  $\Lambda$ ) and a tangential friction impulse ( $F_t$ ) along their respective lines of action. Because the screws in 10 are structured as Plücker lines, scaling them by scalar impulses generates both the 3D contact forces and their induced 3D torques about the center of mass. Using the Coulomb friction model with  $\mu$  (where  $F_t = \mu\Lambda$ ), the dual wrench is:

$$\hat{\mathcal{W}} = \Lambda\hat{\mathbf{s}}_n + \mu\Lambda\hat{\mathbf{s}}_t = \Lambda(\hat{\mathbf{s}}_n + \mu\hat{\mathbf{s}}_t). \quad (11)$$

To determine the scalar magnitude  $\Lambda$ , we apply Newton's Law of Restitution, *i.e.*, the post-impact relative velocity along the normal direction  $v_n^+$  is related to the pre-impact velocity  $v_n^-$  by the coefficient of restitution  $e$  with  $v_n^+ = -ev_n^-$ . In dual

algebra, the projection of a twist  $\hat{\xi}$  onto a screw axis  $\hat{\mathbf{s}}$  is given by the scalar part of the dual dot product  $v_n = \langle \hat{\xi}, \hat{\mathbf{s}}_n \rangle$ . Projecting the dual quaternion reset law (9) onto the normal screw  $\hat{\mathbf{s}}_n$  yields

$$\langle \hat{\xi}^+, \hat{\mathbf{s}}_n \rangle = \langle \hat{\xi}^-, \hat{\mathbf{s}}_n \rangle + \langle \mathcal{M}^{-1}(\hat{\mathcal{W}}), \hat{\mathbf{s}}_n \rangle \quad (12a)$$

$$\Rightarrow -e\langle \hat{\xi}^-, \hat{\mathbf{s}}_n \rangle = \langle \hat{\xi}^-, \hat{\mathbf{s}}_n \rangle + \Lambda\langle \mathcal{M}^{-1}(\hat{\mathbf{s}}_n + \mu\hat{\mathbf{s}}_t), \hat{\mathbf{s}}_n \rangle \quad (12b)$$

To solve for  $\Lambda$ , we adopt the standard decoupled assumption [6], [17], where the frictional impulse does not instantaneously affect the compression along the normal axis, used as well in the standard formulation in (2). Mathematically, this implies neglecting the cross-coupling term:

$$\mu\langle \mathcal{M}^{-1}(\hat{\mathbf{s}}_t), \hat{\mathbf{s}}_n \rangle \approx 0 \quad (13)$$

Applying this simplification yields the final closed-form expression for the impulse magnitude:

$$\Lambda = \frac{-(1+e)\langle \hat{\xi}^-, \hat{\mathbf{s}}_n \rangle}{\langle \mathcal{M}^{-1}(\hat{\mathbf{s}}_n), \hat{\mathbf{s}}_n \rangle} \quad (14)$$

To determine the final post-impact state, the computed impulse magnitude  $\Lambda$  from Eq. (14) is first substituted into Eq. (11) to formulate the total collision wrench  $\hat{\mathcal{W}}$ . Applying this wrench to the update law in Eq. (9) directly yields the post-impact spatial twist  $\hat{\xi}^+$ . We provide a visual representation of this dual quaternion reset sequence in Figure 2.

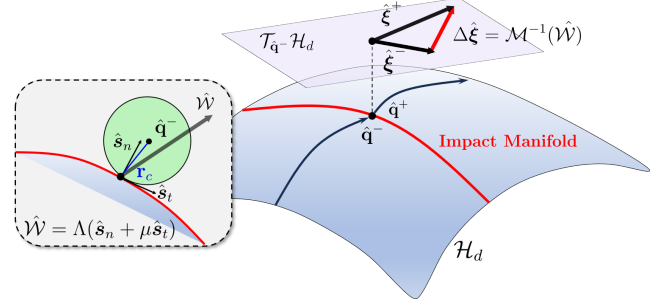


Fig. 2: Geometric interpretation of the Dual Quaternion Reset Map. The reset map in (9) is solved directly on the dual manifold.

**Proposition 1.** The dual quaternion reset map is mathematically equivalent to the standard matrix reset map, *i.e.*,  $\mathcal{R} \equiv \hat{\mathcal{R}}$ .

**Proof.** First, consider the numerator of (14). The dual dot product  $\langle \hat{\xi}^-, \hat{\mathbf{s}}_n \rangle$  projects the spatial twist onto the normal screw axis. This operation directly evaluates the linear velocity of the contact point along the collision normal, which is kinematically equivalent to the classical formulation:

$$\langle \hat{\xi}^-, \hat{\mathbf{s}}_n \rangle \equiv (\mathbf{v}_c^-)^\top \mathbf{n} \quad (15)$$

Next, consider the denominator of Eq. (14), denoted  $\rho_{DQ}$ . Recalling the definition of the inverse dual inertia operator, we evaluate its action on the normal screw as  $\mathcal{M}^{-1}(\hat{\mathbf{s}}_n) = \mathbf{J}^{-1}(\mathbf{r}_c \times \mathbf{n}_B) + \varepsilon(m^{-1}\mathbf{n}_B)$ . Expanding the dual dot product  $\rho_{DQ}$ , with  $\mathbf{n}_B^\top \mathbf{n}_B = 1$ , yields:

$$\rho_{DQ} = (\mathbf{r}_c \times \mathbf{n}_B) \cdot \mathbf{J}^{-1}(\mathbf{r}_c \times \mathbf{n}_B) + m^{-1} \quad (16)$$

By expressing the contact normal in the body frame as  $\mathbf{n}_B = \mathbf{R}^\top \mathbf{n}$ , the effective inverse mass  $\rho$  in Eq. (3) can be expanded as:

$$\rho = \mathbf{n}_B^\top [\mathbf{J}^{-1}(\mathbf{r}_c \times \mathbf{n}_B) \times \mathbf{r}_c] + \mathbf{n}_B^\top (m^{-1} \mathbf{n}_B) \quad (17a)$$

$$= (\mathbf{r}_c \times \mathbf{n}_B)^\top \mathbf{J}^{-1}(\mathbf{r}_c \times \mathbf{n}_B) + m^{-1} \quad (17b)$$

Therefore, we have  $\rho_{DQ} \equiv \rho$ . The effective collision inertia is identical.

The discrete state update is  $\Delta \hat{\xi} = \mathcal{M}^{-1}(\hat{\mathcal{W}})$ . Using the total impulse in the body frame  $\lambda_B = \Lambda(\mathbf{n}_B + \mu \mathbf{t}_B)$ , the dual wrench  $\hat{\mathcal{W}}$  can be developed as:

$$\hat{\mathcal{W}} = (\mathbf{r}_c \times \lambda_B) + \varepsilon \lambda_B. \quad (18)$$

Applying the inverse mass operator  $\mathcal{M}^{-1}(\cdot)$  to this wrench gives the following twist update

$$\Delta \hat{\xi} = \underbrace{\mathbf{J}^{-1}(\mathbf{r}_c \times \lambda_B)}_{\Delta \omega} + \varepsilon \underbrace{(m^{-1} \lambda_B)}_{\Delta \mathbf{v}_B}. \quad (19)$$

The angular update  $\Delta \omega$  matches the standard model in (2) exactly. For the linear update, the standard model updates inertial velocity  $\mathbf{v}$ . The DQ model updates body velocity  $\mathbf{v}_B$  as

$$\Delta \mathbf{v} = \mathbf{R}(\Delta \mathbf{v}_B) = \mathbf{R}(m^{-1} \lambda_B) = m^{-1} \lambda. \quad (20)$$

Since the reset update is expressed directly in the spatial twist associated with the dual quaternion representation, the post-impact state remains on the manifold without intermediate coordinate transformations. Therefore, the proposed reset map is mathematically equivalent to the classical model in (2) while maintaining geometric consistency across jumps. ■

**Remark 1.** Classical reset implementations suffer from the decoupled treatment of translation and rotation in  $\mathbb{R}^3 \times SO(3)$ . This separation forces the controller to reconcile discontinuities across orthogonal metric spaces during hybrid events, potentially inducing undesired control inputs to underactuated systems [4]. Our approach represents the pose as a single entity on  $SE(3)$  via dual quaternions. By updating the spatial twist directly in dual algebra, the proposed reset map ensures discrete jumps remain within the manifold. This alignment of the reset operation with the controller's geometry allows impact-induced momentum changes to be resolved through unified geometric feedback laws.

### C. Dual Quaternion Impact Recovery Control

To avoid actuator saturation during collision events, we implement an admittance-based recovery strategy directly on the dual quaternion manifold, adapting the classical non dual formulations seen in [3], [18]. At impact time  $t_c$ , the closed-form impulse magnitude  $\Lambda$  in (14) and impulsive wrench  $\hat{\mathcal{W}}$  in (11) are used to compute the post-impact twist via the dual reset map in (9). We define the following dual admittance gain  $\hat{\Gamma} \in \mathbb{R}^{3 \times 3} + \varepsilon \mathbb{R}^{3 \times 3}$

$$\hat{\Gamma} = \Gamma_\omega + \varepsilon \Gamma_v, \quad \Gamma_i = \text{diag}(\gamma_{i,x}, \gamma_{i,y}, \gamma_{i,y}) \quad (21)$$

Here,  $\Gamma_\omega, \Gamma_v \in \mathbb{R}^{3 \times 3}$  are positive-definite diagonal matrices containing the independent control gains for the rotational and

translational axes. We scale the post-impact twist to obtain the braking displacement in the Lie algebra as follows

$$\hat{\delta} = \hat{\Gamma} \circ \hat{\xi}^+ = \Gamma_\omega \omega^+ + \varepsilon \Gamma_v \mathbf{v}_B^+. \quad (22)$$

The displacement  $\hat{\delta}$  is mapped to the configuration manifold via the dual exponential  $\hat{\mathbf{q}}_\Delta = \exp(\frac{1}{2} \hat{\delta})$  [15]. The recovery setpoint  $\hat{\mathbf{q}}_d$  and configuration error  $\hat{\mathbf{q}}_e$  are defined as

$$\hat{\mathbf{q}}_d = \hat{\mathbf{q}}_\Delta \otimes \hat{\mathbf{q}}(t_c) \quad (23a)$$

$$\hat{\mathbf{q}}_e = \hat{\mathbf{q}}_d^* \otimes \hat{\mathbf{q}} = \mathbf{q}_e + \varepsilon \frac{1}{2} \mathbf{p}_e \otimes \mathbf{q}_e \quad (23b)$$

Shifting the reference trajectory introduces virtual compliance, allowing the UAV to yield to the collision. This avoids tracking errors associated with rigid setpoints, smoothly dissipating impact energy while keeping motor commands bounded.

**Remark 2.** Our formulation shares the same objective as classical admittance control [3], [18] by inducing post-impact compliance in the system and generalizes classical admittance control to  $SE(3)$ . While classical admittance decouples contact forces and torques, risking physically conflicting reference trajectories during impacts, our approach processes the unified dual wrench. By enforcing coupled screw motion, the outer-loop setpoint inherently accounts for momentum transfer. This guarantees  $SE(3)$ -consistent compliance and enhances recovery performance without requiring custom inner-loop modifications.

**Hybrid Lyapunov Stability** (The extend version of the proof is shown in Appendix VI-A)

Defining the state  $x = (\hat{\mathbf{q}}, \hat{\xi})$ , we model the closed-loop recovery system as a hybrid dynamical system  $\mathcal{H} = (F, \mathcal{C}, \mathcal{D}, \hat{\mathcal{R}})$  satisfying standard basic conditions [19]. The flow and jump sets are  $\mathcal{C} = \{x \mid \phi(\hat{\mathbf{q}}) > 0\}$  and  $\mathcal{D} = \{x \mid \phi(\hat{\mathbf{q}}) \leq 0\}$ , where  $\phi$  is the signed distance to the contact surface. Since  $e \in [0, 1[$  ensures bounded kinetic energy dissipation at each impact, Zeno executions are excluded. Using (23b), with  $q_e^w$  and  $\mathbf{q}_e^v$  being the scalar and vector parts of  $\mathbf{q}_e$ , the continuous dynamics  $F$  from Eq. 4 are governed by the control law:

$$\hat{\mathbf{F}}_a = -\hat{\mathbf{F}}_g + \hat{\xi} \times^* \hat{\mathbf{H}} - \underbrace{(k_q \mathbf{q}_e^v + \varepsilon k_p \mathbf{p}_e)}_{\hat{\mathbf{e}}} - \mathbf{K}_d \circ \hat{\xi} \quad (24)$$

which cancels nonlinear coupling and injects dual damping via  $\mathbf{K}_d > 0$ .

**Proposition 2.** The closed-loop hybrid system achieves Hybrid Lyapunov stability at  $\mathcal{A} = \{x \mid \hat{\mathbf{q}}_e = \mathbf{1}, \hat{\xi} = \mathbf{0}\}$ .

**Proof.** Consider the candidate Lyapunov function

$$V(x) = \underbrace{2k_q(1 - q_e^w) + \frac{1}{2}k_p \|\mathbf{p}_e\|^2}_{V_{pos}} + \underbrace{\frac{1}{2} \langle \hat{\xi}, \mathcal{M}(\hat{\xi}) \rangle}_{V_{kin}} \quad (25)$$

which is positive definite with respect to  $\mathcal{A}$ .

*Flow condition* ( $x \in \mathcal{C}$ ). Since the reference pose is constant during free flight, differentiating  $V$  along the flow gives

$$\dot{V} = \langle \hat{\mathbf{e}}, \hat{\xi} \rangle + \langle \hat{\xi}, \hat{\mathbf{F}}_a + \hat{\mathbf{F}}_g - \hat{\xi} \times^* \hat{\mathbf{H}} \rangle. \quad (26)$$

Substituting (24) yields cancellation of gravitational, gyroscopic, and potential gradient terms. The remaining term is

$$\dot{V} = -\langle \hat{\xi}, \mathbf{K}_d \circ \hat{\xi} \rangle \leq 0 \quad (27)$$

establishing non-increasing energy along flows.

*Jump condition* ( $x \in \mathcal{D}$ ). At impact,  $\Delta V_{pos} = 0$  and the change in kinetic energy satisfies

$$\Delta V_{kin} = \langle \hat{\xi}^-, \hat{W} \rangle + \frac{1}{2} \langle \hat{W}, \mathcal{M}^{-1}(\hat{W}) \rangle \quad (28)$$

Substituting  $\hat{W}_n = \Lambda \hat{s}_n$  and using the restitution relation gives

$$\Delta V_{kin,n} = -\frac{1}{2} \Lambda^2 \langle \hat{s}_n, \mathcal{M}^{-1}(\hat{s}_n) \rangle \left( \frac{1-e}{1+e} \right) \quad (29)$$

Since  $\mathcal{M} \succ 0$  and  $e \in [0, 1]$ , this is strictly negative. Coulomb friction ensures  $\Delta V_{kin,t} \leq 0$ , yielding total dissipation  $\Delta V_{kin} = -E_{diss} < 0$ .

The setpoint update introduces a bounded pose shift  $\hat{\mathbf{q}}_\Delta = \exp(\hat{\delta}/2)$ . For sufficiently small braking gains  $(\Gamma_\omega, \Gamma_v)$  satisfying

$$\frac{1}{4} k_q \|\Gamma_\omega \omega^+\|^2 + \frac{1}{2} k_p \|\Gamma_v \mathbf{v}_B^+\|^2 < E_{diss} + V_{pos}(\hat{\mathbf{q}}_e^-) \quad (30)$$

the total change of the Lyapunov function at impact satisfies  $\Delta V < 0$ . Since  $\dot{V} \leq 0$  on  $\mathcal{C}$  and  $\Delta V < 0$  on  $\mathcal{D}$ , Lyapunov stability of the closed-loop hybrid system follows [19]. ■

**Remark 3.** When selecting  $(\Gamma_v, \Gamma_\omega)$ , we can introduce a weight  $\alpha \in [0, 1]$  to distribute the energy budget, which yields explicit upper bounds:

$$\|\Gamma_\omega\|_2 < \sqrt{\frac{4\alpha E(\hat{\mathbf{q}}_e^-)}{k_q \|\omega^+\|^2}}, \quad \|\Gamma_v\|_2 < \sqrt{\frac{2(1-\alpha)E(\hat{\mathbf{q}}_e^-)}{k_p \|\mathbf{v}_B^+\|^2}} \quad (31)$$

with  $E(\hat{\mathbf{q}}_e^-) = E_{diss} + V_{pos}(\hat{\mathbf{q}}_e^-)$ . For non-perfectly elastic impacts ( $e < 1$ ), kinetic dissipation guarantees  $E_{diss} > 0$ , ensuring these bounds remain strictly positive.

#### IV. NUMERICAL VALIDATION AND SIMULATION

In this section, we evaluate the performance of the dual quaternion (DQ) recovery framework of Section III-C against a non dual recovery baseline inspired by [3], [18].

##### A. Computational Complexity Analysis

We begin by evaluating the computational advantages of the proposed DQ reset map. We define the computational cost function  $C(\cdot)$  as the total floating-point operations (FLOPs) needed to generate the reset map, assigning unit weights to additions and multiplications [11]. We compare three impulse determination strategies: the world-frame *Inertial Formulation*, the body-frame *Matrix Formulation*, and our *DQ Formulation*. As shown in Table I, the DQ approach achieves a 25% FLOP reduction over the optimized matrix baseline.

C++ benchmarks (-O3) on a Raspberry Pi 5 (quad-core Arm Cortex-A76, 2.4 GHz) validated these gains, demonstrating a 24% execution time reduction. This latency drop expands the timing margin for concurrent autonomy threads on shared UAV hardware. Additionally, operating on 8-element dual quaternion arrays rather than 12 element matrix-vector pairs maximizes cache coherency and reduces stack pressure, which is critical for Real-Time Operating System (RTOS) stability.

TABLE I: Computational Cost Comparison

	Inertial Form.	Matrix Form.	DQ Form.
Rotation	$\mathbf{R}$	$\mathbf{R}$	N/A
Frame	N/A	Mat-Vec Mult	Quaternion
Inertia	Rot. Tensor	Const. Diag	Const. Diag
Total FLOPs	$\approx 144$	$\approx 69$	$\approx 52$
Relative Cost	209%	100% (Baseline)	75%

##### B. Validation Simulations

To validate the controller's stability and energy dissipation capabilities, we simulated a rigid-body collision in MATLAB. The quadrotor is subjected to an collision ( $e = 0.7$ ,  $\mu = 0.3$ ) and tasked to stabilize to a safe hovering setpoint.

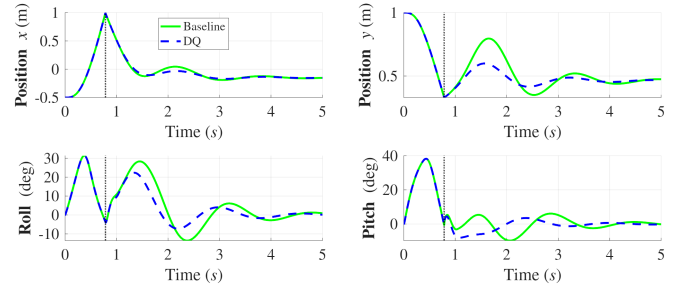


Fig. 3: MATLAB simulation results for an impact velocity of 2 m/s: position and attitude responses to an idealized impulse.

As shown in Fig. 3, while both controllers achieve post-impact stability, their transient performance differs. The traditional controller's decoupled approach results in sustained attitude oscillations and longer settling time. Our method, by coupling linear and angular momentum, prioritizes total momentum dissipation. This geometric coupling enables more efficient energy dissipation and faster convergence to a stable 6-DOF recovery state.

##### C. High-Fidelity Physics Simulation

Robustness was evaluated in MuJoCo [7] using soft-constraint LCP solvers that resolve coupled normal and frictional forces. Unlike the decoupled assumption in (13), MuJoCo generates complex cross-coupled torques that act as unmodeled disturbances. With identical free-flight tuning, this setup tests the controller's robustness to unmodeled cross-coupled contact dynamics.

We compare the proposed dual quaternion (DQ) recovery framework with the baseline using continuous  $L_2$  position error and total kinetic energy decay following impact. In addition to the single run in MuJoCo as shown in Fig. 4, we also conducted a Monte Carlo simulation over twenty ( $N = 20$ ) initial positions of the drone at a constant altitude to assess robustness.

Figure 4 shows that these off-axis impact torques cause the baseline controller [3], [18] to lose lateral authority, resulting in significant cross-coupling and persistent pitch/roll oscillations lasting nearly 4 s. On the other hand, the DQ controller uses a unified geometric entity. It bounds lateral cross-coupling that attenuates asymmetric oscillations. By operating natively

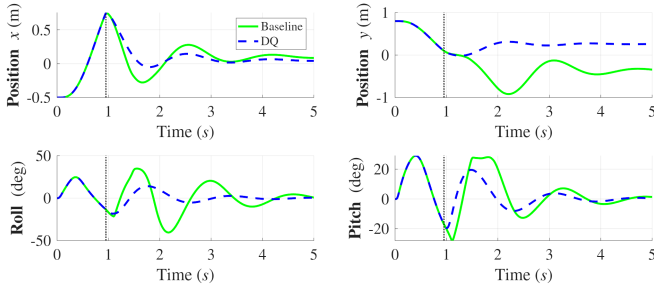


Fig. 4: MuJoCo simulation results for an impact velocity of 2 m/s: high-fidelity kinematic response demonstrating the significant lateral cross-coupling of the baseline controller.

on  $SE(3)$ , the DQ-based recovery controller inherently bounds lateral cross-coupling and aligns the recovery twist with the physical spin, attenuating asymmetric oscillations. As detailed in Table II, this leads to a 41.2% reduction in peak kinetic energy ( $E_k$ ) and a 23.2% reduction in peak  $L_2$  tracking error

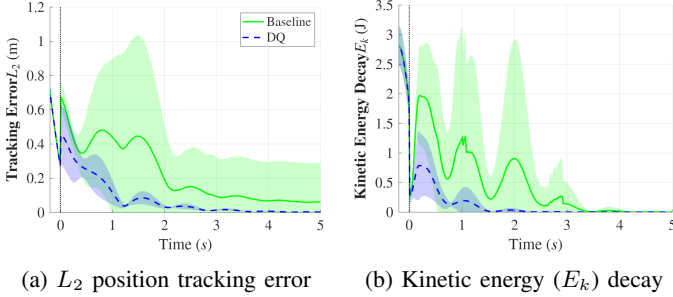


Fig. 5: Monte Carlo results in MuJoCo during the post-impact recovery phase.

In Monte Carlo trials, the DQ method improves the  $L_2$  RMSE by 56.3%, maintaining tightly bounded lateral deviation without prolonged oscillations, as shown in Fig. 5a. By resolving the impulse directly in the dual algebra, the DQ method yields a better damped energy decay (Fig. 5b). This physical compliance drives a 61.1% reduction in mean peak  $E_k$  and a 29.5% reduction in settling time, as shown in Table II.

TABLE II: Comparisons of Post-Impact Recovery Metrics

Metric	Single Run Improv.	Monte Carlo Improv.
Peak $L_2$ error (m)	23.2%	21.1%
$L_2$ RMSE (m)	56.6%	56.3%
Peak $E_k$ (J)	41.2%	61.1%
Settling Time (s)	22.7%	29.5%

## V. CONCLUSION

This article presented a dual quaternion reset map to resolve rigid-body aerial impacts directly on the  $SE(3)$  manifold. By extending Newton’s restitution law to dual screws, we derived a closed-form impulse update that functions as an  $SE(3)$  momentum reset, formally equivalent to the classical Newton formulation while preserving manifold consistency. We leveraged this formulation to develop a hybrid recovery controller

with guaranteed Lyapunov stability and strict kinetic energy dissipation across impacts. Numerical validations showed a 24% reduction in computational overhead relative to matrix-based baselines. High-fidelity simulations demonstrated that resolving impacts on the dual algebra inherently couples linear and angular momentum recovery, yielding superior damping of post-impact oscillations compared to its non-dual counterpart.

Future work will focus on extending these theoretical stability guarantees to multi-point contact scenarios and adaptive restitution estimation on  $SE(3)$ , before integrating this manifold-consistent structure into model predictive control frameworks for impact-aware planning in cluttered environments.

## REFERENCES

- Ruggiero, F., Lippiello, V., and Ollero, A., “Aerial manipulation: A literature review,” *IEEE Robotics and Automation Letters*, vol. 3, no. 3, pp. 1957–1964, 2018.
- Patnaik, K., Saravanakumaran, A. A. P., and Zhang, W., “Tactile-based exploration, mapping, and navigation with collision-resilient aerial vehicles,” *IEEE/ASME Transactions on Mechatronics*, vol. 30, no. 4, pp. 2910–2918, 2025.
- Bredenbeck, A., Yang, T., Hamaza, S., and Mueller, M. W., “A tactile feedback approach to path recovery after high-speed impacts for collision-resilient drones,” *Drones*, vol. 9, no. 11, 2025.
- Lee, T., Leok, M., and McClamroch, N. H., “Geometric tracking control of a quadrotor uav on  $se(3)$ ,” in *49th IEEE Conference on Decision and Control (CDC)*, 2010, pp. 5420–5425.
- Mirtich, B. and Canny, J., “Impulse-based simulation of rigid bodies,” in *Proceedings of the 1995 Symposium on Interactive 3D Graphics*, ser. I3D ’95. New York, NY, USA: Association for Computing Machinery, 1995, p. 181–ff.
- Stewart, D. E., “Rigid-body dynamics with friction and impact,” *SIAM Review*, vol. 42, no. 1, pp. 3–39, 2000.
- Todorov, E., Erez, T., and Tassa, Y., “Mujoco: A physics engine for model-based control,” in *2012 IEEE/RSJ International Conference on Intelligent Robots and Systems*. IEEE, 2012, pp. 5026–5033.
- Abazari, A., Kumar, Y., Patnaik, K., and Zhang, W., “Dynamic collision-inclusive modeling of a multirotor aerial vehicle using linear complementarity systems,” in *2025 American Control Conference (ACC)*, 2025.
- Clifford, “Preliminary sketch of biquaternions,” *Proceedings of The London Mathematical Society*, pp. 381–395, 1871.
- McCarthy, J. M., *An introduction to theoretical kinematics / J. Michael McCarthy*. Cambridge, Mass: MIT Press, 1990.
- Wang, X. and Zhu, H., “On the comparisons of unit dual quaternion and homogeneous transformation matrix,” *Advances in Applied Clifford Algebras*, vol. 24, 03 2014.
- Filipe, N. and Tsiotras, P., “Adaptive position and attitude-tracking controller for satellite proximity operations using dual quaternions,” *Journal of Guidance, Control, and Dynamics*, vol. 38, 2015.
- Cui, C., Qi, L., Chen, H., and Wang, X., “A dual quaternion control law for formation control of multiple 3-d rigid bodies,” 2025.
- Marciano, H. N., Dourado Villa, D. K., Sarcinelli-Filho, M., and Giribet, J. I., “Dual quaternion-based control for a leader-follower formation of two quadrotors,” in *2024 International Conference on Unmanned Aircraft Systems (ICUAS)*, 2024, pp. 732–739.
- Recalde, L. F., Agrawal, D., Arrizabalaga, J., and Li, G., “Dq-nmpc: Dual-quaternion nmpc for quadrotor flight,” *IEEE Robotics and Automation Letters*, pp. 1–8, 2025.
- Brodsky, V. and Shoham, M., “Dual numbers representation of rigid body dynamics,” *Mechanism and Machine Theory*, vol. 34, no. 5, 1999.
- Jia, Y.-B., *Energy-Based Modeling of Tangential Compliance in 3-Dimensional Impact*. Berlin, Heidelberg: Springer Berlin Heidelberg, 2011, pp. 267–284.
- Patnaik, K., Mishra, S., Chase, Z., and Zhang, W., “Collision recovery control of a foldable quadrotor,” in *2021 IEEE/ASME International Conference on Advanced Intelligent Mechatronics (AIM)*, 2021.
- Goebel, R., Sanfelice, R. G., and Teel, A. R., *Hybrid Dynamical Systems: Modeling, Stability, and Robustness*. Princeton, NJ, USA: Princeton University Press, 2012.

## VI. APPENDIX

## A. Extended Hybrid Lyapunov Stability Proof

In this appendix, we provide the complete mathematical derivation of the Hybrid Lyapunov stability conditions for the proposed dual quaternion closed-loop recovery system.

1) *System Definition and Lyapunov Candidate*: We define the hybrid system state as  $x = (\hat{\mathbf{q}}_e, \hat{\xi})$ , where  $\hat{\mathbf{q}}_e$  is the dual quaternion pose error and  $\hat{\xi}$  is the body twist. The hybrid dynamical system is defined as  $\mathcal{H} = (F, \mathcal{C}, \mathcal{D}, \hat{\mathcal{R}})$ .

We consider the candidate Lyapunov function defined as:

$$V(x) = \underbrace{2k_q(1 - q_e^w) + \frac{1}{2}k_p\|\mathbf{p}_e\|^2}_{V_{pos}} + \underbrace{\frac{1}{2}\langle \hat{\xi}, \mathcal{M}(\hat{\xi}) \rangle}_{V_{kin}} \quad (32)$$

where  $q_e^w$  is the scalar real part of the real error quaternion,  $\mathbf{p}_e$  is the translational error, and  $\mathcal{M} > 0$  is the dual inertia matrix. By definition,  $V(x) \geq 0$  and  $V(x) = 0$  if and only if  $x \in \mathcal{A} = \{x \mid \hat{\mathbf{q}}_e = \mathbf{1}, \hat{\xi} = \mathbf{0}\}$ .

2) *Continuous Dynamics (Flow Set C)*: During free flight, the state lies in the flow set  $\mathcal{C} = \{x \mid \phi(\hat{\mathbf{q}}) > 0\}$ . The time derivative of the Lyapunov function is  $\dot{V} = \dot{V}_{pos} + \dot{V}_{kin}$ .

Taking the time derivative of  $V_{pos}$  and utilizing the dual quaternion kinematic propagation  $\dot{\hat{\mathbf{q}}}_e = \frac{1}{2}\hat{\mathbf{q}}_e \otimes \hat{\xi}$ , we obtain the inner product with the generalized error vector  $\hat{\mathbf{e}}$ :

$$\dot{V}_{pos} = \langle \hat{\mathbf{e}}, \hat{\xi} \rangle, \quad \text{where } \hat{\mathbf{e}} \triangleq k_q \mathbf{q}_e^v + \varepsilon k_p \mathbf{p}_e \quad (33)$$

Differentiating the kinetic energy yields:

$$\dot{V}_{kin} = \langle \hat{\xi}, \mathcal{M}(\dot{\hat{\xi}}) \rangle = \langle \hat{\xi}, \hat{\mathbf{F}}_a + \hat{\mathbf{F}}_g - \hat{\xi} \times^* \mathcal{M}(\hat{\xi}) \rangle \quad (34)$$

By the definition of the dual co-adjoint operator, the gyroscopic term is strictly orthogonal to the twist, meaning  $\langle \hat{\xi}, \hat{\xi} \times^* \mathcal{M}(\hat{\xi}) \rangle = 0$ . Substituting the proposed control law  $\hat{\mathbf{F}}_a = -\hat{\mathbf{F}}_g + \hat{\xi} \times^* \mathcal{M}(\hat{\xi}) - \hat{\mathbf{e}} - \mathbf{K}_d \circ \hat{\xi}$  into  $\dot{V}_{kin}$  yields:

$$\dot{V} = \langle \hat{\mathbf{e}}, \hat{\xi} \rangle + \langle \hat{\xi}, -\hat{\mathbf{e}} - \mathbf{K}_d \circ \hat{\xi} \rangle \quad (35)$$

The potential gradient terms  $\langle \hat{\mathbf{e}}, \hat{\xi} \rangle$  cancel exactly, leaving:

$$\dot{V} = -\langle \hat{\xi}, \mathbf{K}_d \circ \hat{\xi} \rangle \leq 0 \quad (36)$$

Because  $\mathbf{K}_d > 0$ ,  $\dot{V} \leq 0$  strictly holds for all  $x \in \mathcal{C}$ , proving energy non-increase along continuous flows.

3) *Impact Dynamics (Jump Set D)*: At the instant of impact, the system enters the jump set  $\mathcal{D} = \{x \mid \phi(\hat{\mathbf{q}}) \leq 0\}$ . The total change in the Lyapunov function across the discrete jump is  $\Delta V = V(x^+) - V(x^-) = \Delta V_{pos} + \Delta V_{kin}$ .

**Kinetic Energy Dissipation** The instantaneous change in kinetic energy is:

$$\Delta V_{kin} = \frac{1}{2}\langle \hat{\xi}^+, \mathcal{M}(\hat{\xi}^+) \rangle - \frac{1}{2}\langle \hat{\xi}^-, \mathcal{M}(\hat{\xi}^-) \rangle \quad (37)$$

Using the momentum update  $\mathcal{M}(\hat{\xi}^+) = \mathcal{M}(\hat{\xi}^-) + \hat{\mathcal{W}}$ , this expands to:

$$\Delta V_{kin} = \langle \hat{\xi}^-, \hat{\mathcal{W}} \rangle + \frac{1}{2}\langle \hat{\mathcal{W}}, \mathcal{M}^{-1}(\hat{\mathcal{W}}) \rangle \quad (38)$$

Substituting the normal wrench component  $\hat{\mathcal{W}}_n = \Lambda \hat{\mathbf{s}}_n$  and applying the kinematic restitution constraint  $\langle \hat{\mathbf{s}}_n, \hat{\xi}^+ \rangle = -e \langle \hat{\mathbf{s}}_n, \hat{\xi}^- \rangle$ , the normal energy change resolves to:

$$\Delta V_{kin,n} = -\frac{1}{2}\Lambda^2 \langle \hat{\mathbf{s}}_n, \mathcal{M}^{-1}(\hat{\mathbf{s}}_n) \rangle \left( \frac{1-e}{1+e} \right) \quad (39)$$

For any restitution  $e \in [0, 1[$ , this term is strictly negative. Combined with strictly dissipative Coulomb friction limits  $\Delta V_{kin,t} \leq 0$ , the total kinetic energy change is strictly dissipative:

$$\Delta V_{kin} = -E_{diss} < 0 \quad (40)$$

**Potential Energy Bound via Admittance Setpoint Shift** To dissipate rotational energy, the controller induces a bounded reference pose shift  $\hat{\mathbf{q}}_\Delta = \exp(\hat{\delta}/2)$ , where the spatial twist command is parameterized by  $\hat{\delta} = \Gamma_\omega \omega^+ + \varepsilon \Gamma_v \mathbf{v}_B^+$ .

By the triangle inequality on  $SE(3)$ , the post-impact potential energy is bounded by the sum of the pre-impact potential energy and the "artificial" potential energy injected by the setpoint shift:

$$V_{pos}^+ \leq V_{pos}^- + V_{pos}(\hat{\mathbf{q}}_\Delta) \quad (41)$$

To evaluate  $V_{pos}(\hat{\mathbf{q}}_\Delta)$ , we use the small-angle approximation of the exponential map on  $SE(3)$  for small gain parameters. The scalar real part of  $\hat{\mathbf{q}}_\Delta$  is  $q_\Delta^w = \cos(\|\delta_\omega\|/2) \approx 1 - \frac{1}{8}\|\delta_\omega\|^2$ . The translational part is approximately  $\mathbf{p}_\Delta \approx \delta_v$ . Therefore:

$$\begin{aligned} V_{pos}(\hat{\mathbf{q}}_\Delta) &= 2k_q \left( \frac{1}{8}\|\delta_\omega\|^2 \right) + \frac{1}{2}k_p \|\delta_v\|^2 \\ &= \frac{1}{4}k_q \|\Gamma_\omega \omega^+\|^2 + \frac{1}{2}k_p \|\Gamma_v \mathbf{v}_B^+\|^2 \end{aligned} \quad (42)$$

To guarantee total stability across the jump ( $\Delta V < 0$ ), the injected potential energy must be strictly less than the dissipated kinetic energy:

$$V_{pos}(\hat{\mathbf{q}}_\Delta) < -\Delta V_{kin} \implies V_{pos}(\hat{\mathbf{q}}_\Delta) < E_{diss} \quad (43)$$

A more conservative, globally valid limit considers the total system energy budget  $E(\hat{\mathbf{q}}_e^-) = E_{diss} + V_{pos}^-$ , yielding the condition:

$$\frac{1}{4}k_q \|\Gamma_\omega \omega^+\|^2 + \frac{1}{2}k_p \|\Gamma_v \mathbf{v}_B^+\|^2 < E(\hat{\mathbf{q}}_e^-) \quad (44)$$

4) *Admittance Gain Synthesis*: To systematically satisfy the bounded shift condition, we introduce a scaling parameter  $\alpha \in (0, 1)$  to allocate the allowable energy budget between rotational and translational recovery. By decoupling the inequality into two independent bounds:

$$\frac{1}{4}k_q \|\Gamma_\omega \omega^+\|^2 < \alpha E(\hat{\mathbf{q}}_e^-) \quad (45)$$

$$\frac{1}{2}k_p \|\Gamma_v \mathbf{v}_B^+\|^2 < (1 - \alpha) E(\hat{\mathbf{q}}_e^-) \quad (46)$$

Isolating the norms of the braking gain matrices yields the explicit upper bounds:

$$\|\Gamma_\omega\|_2 < \sqrt{\frac{4\alpha E(\hat{\mathbf{q}}_e^-)}{k_q \|\omega^+\|^2}}, \quad \|\Gamma_v\|_2 < \sqrt{\frac{2(1-\alpha)E(\hat{\mathbf{q}}_e^-)}{k_p \|\mathbf{v}_B^+\|^2}} \quad (47)$$

Since  $\dot{V} \leq 0$  for all flows  $x \in \mathcal{C}$ , and  $\Delta V < 0$  for all jumps  $x \in \mathcal{D}$  strictly under these gain bounds, the origin  $\mathcal{A}$  is asymptotically Hybrid Lyapunov stable. ■